OPEN

NPG Asia Materials (2017) 9, e405; doi:10.1038/am.2017.107
www.nature.com/am

ORIGINAL ARTICLE

Micron-thick highly conductive PEDOT films synthesized via self-inhibited polymerization: roles of anions

Wei Shi[1,2], Qin Yao[1], Sanyin Qu[1], Hongyi Chen[1,2], Tiansong Zhang[1] and Lidong Chen[1,3]

The inhibitor-dependent poly(3,4-ethylenedioxythiophene) (PEDOT) fabrication suffers major problems in the areas of controllability and film thickness. In this work, we found that anions play a key role in both the polymerization and the structure of PEDOT. As a precursor, anions greatly influence the reaction rate and oxidant solubility. In its role as a counter-ion, the anions also affect chain conductance and crystal growth. With these behaviors in mind, a self-inhibited polymerization approach using novel oxidants with appropriate anions was successfully developed to facilitate the fabrication of high quality *in situ* polymerized PEDOT films and solve the thickness limitation problem. Inhibitor-free heavy oxidative solutions with weakly basic anions enable the spin-coating of thick and homogeneous oxidant layers and also effectively inhibit both the crystallization of the oxidant and H^+ formation throughout the polymerization process. PEDOT: dodecylbenzenesulfonate (PEDOT:DBSA) exhibits the highest performance among all candidates due to its appropriate anion basicity and low steric effect. An extremely high doping level of 42.9% is achieved, and an electrical conductivity of ~ 1100 S cm^{-1} is successfully maintained for film thicknesses between 310 nm and 1.79 μm. In addition, the thermoelectric power factor (RT) for pristine films was improved to 77.2 μW mK^{-2} from 69.6 μW mK^{-2} by the dedoping treatment. This study provides a new approach for fabricating high performance PEDOT thick films using anion-based design.
NPG Asia Materials (2017) **9,** e405; doi:10.1038/am.2017.107; published online 14 July 2017

INTRODUCTION

Thermoelectric (TE) materials realize direct conversion between heat and electricity, which can be used in refrigeration and power generation. The performance of TE materials is characterized by the ZT value ($S^2\sigma T/\kappa$) or power factor ($S^2\sigma$), where S, σ, T and κ are the Seebeck coefficient, electrical conductivity, absolute temperature and thermal conductivity, respectively. Conducting polymer TE materials possess the advantages of low κ, good flexibility and low cost in comparison with inorganic materials.[1–4] Among them, commercially available PEDOT:polystyrenesulfonate (PEDOT:PSS) has received the most attention due to its excellent water processability and high σ (refs 5–11) and is also widely used as an electrode or conductive adhesive material in applications including solar cells,[12,13] organic light-emitting diodes (OLEDs),[14,15] supercapacitors,[16,17] sensors[18,19] and so on. The PSS polyanion enables the formation of aqueous PEDOT:PSS solutions, which benefits both film printing and the synthesis of hybrid materials. However, such PSS-based processes also experience difficulties with performance optimization. For example, the insulating PSS lamellas remain in the polymer matrix,[20,21] resulting in an amorphous polymer[22] with limited σ and S.[5,9] Compared to PEDOT:PSS, PEDOT doped with small-sized anions (S-PEDOTs), such as tosylate (OTs) or triflate (OTf), have greater potential for electrical applications because of their compact and ordered polycrystalline structure[23] that leads to higher σ and S.[22,24–26] S-PEDOTs often exhibit large $S^2\sigma$ that can be further optimized by tuning the oxidation level.[27–29] However, these high quality films are hard to obtain due to their poor reaction controllability and difficult to put into practical use because of their limited film thickness. The ability to control the polymerization process and the structure of the polymer is currently limited due to the lack of research into the role of the anion, which accounts for a large portion of both PEDOT and its precursor.

S-PEDOTs are prepared by *in situ* polymerization techniques, including solution casting polymerization (CP) and vapor phase polymerization (VPP), using oxidants such as $FeOTs_3$ and $FeOTf_3$. These conventional oxidants are highly acidic and reactive, which makes the polymerization uncontrollable and results in structural defects in the deposited film. Inhibitors are required, and base inhibitors, such as pyridine (Py), are usually used to increase the pH in order to control the reaction rate.[30] However, the unequal

[1]State Key Laboratory of High Performance Ceramics and Superfine Microstructures, Shanghai Institute of Ceramics, Chinese Academy of Sciences, Shanghai, China; [2]University of Chinese Academy of Science, Beijing, China and [3]CAS Key Laboratory of Materials for Energy Conversion, Shanghai Institute of Ceramics, Chinese Academy of Sciences, Shanghai, China
Correspondence: Professor Q Yao or Professor L Chen, State Key Laboratory of High Performance Ceramics and Superfine Microstructures and CAS Key Laboratory of Materials for Energy Conversion, Shanghai Institute of Ceramics, Chinese Academy of Sciences, 1295 Dingxi Road, Shanghai 200050, China.
E-mail: yaoqin@mail.sic.ac.cn or cld@mail.sic.ac.cn
Received 13 February 2017; revised 23 March 2017; accepted 31 March 2017

evaporation of pyridine leads to uneven polymerization and a severe deterioration of σ when fabricating thicker films.[31] In addition to pyridine, copolymer inhibitors, such as poly(ethylene glycol)-block-poly(propylene glycol)-block-poly(ethylene glycol) (PEPG), are also commonly used to reduce the oxidant reactivity through steric effects and suppress the crystallization of oxidants,[22,26–28,32–35] but the copolymer phase remaining inside PEDOT causes the deterioration of σ.[33] For both applications as TE devices and electrode materials, PEDOT films with a reasonable thickness are required. However, OTs and OTf anions have a low affinity for alcohol, which allows only limited (<40 wt%) concentrations in solution and the production of films with low thicknesses of 50–260 nm.[25–33] These oxidants are also easily crystallized during the reaction due to their low solubility, and the crystallized oxidants cause the formation of pin-hole defects in the film.[34] The loading of PEPG further reduces the film thickness due to a severe concentrating effect. A low thickness results in both a high internal resistance that limits the power output as a TE device[36] and a high square resistance that is not viable for electrode materials. Although multiple fabrications could be used to obtain thicker films, that process may not only generate layer–layer interfaces due to the disconnected polymer chains and nonuniformity along the layer growth direction[31,33,34] but also cause the decomposition of the former-step-deposited layers by re-heating.

In this work, we studied three new oxidants, iron(III) dodecylbenzenesulfonate ($FeDBSA_3$), iron(III) butylnaphthalenesulfonate ($FeBNSA_3$) and iron(III) camphorsulfonate ($FeCSA_3$), and used them to synthesize viable thick PEDOT films through self-inhibited polymerization (SIP). We systematically studied the influence of the anion type on the morphology, reactivity, doping level and structure of PEDOT. It was found that oxidants with alcohophilic anions can achieve heavy solutions and prevent the crystallization of oxidants throughout the reaction. The reaction rate can also be effectively controlled by using oxidants with weakly basic anions (WBAs). This self-inhibiting effect ensures the formation of homogeneous thick films without adding harmful inhibitors. Scheme 1 shows a comparison of the SIP route with the conventional route. Due to the low steric effect and a balanced anion basicity that ensure both a controllable reaction and fine chain conductance, PEDOT:DBSA exhibits the best overall electrical performance. Additionally, the $S^2\sigma$ of PEDOT:DBSA was optimized by dedoping treatment. This work presents a facile route to acquire thick and high quality PEDOT films for use in applications.

EXPERIMENTAL PROCEDURES

Materials

EDOT was purchased from Ourchem (Guangzhou, China). Sodium dodecylbenzenesulfonate and dodecylbenzenesulfonic acid were purchased from Aladdin (Shanghai, China). Camphorsulfonic acid, barium hydroxide octahydrate, iron(III) sulfate hydrate, iron(III) chloride hexahydrate, phenylhydrazine and all solvents were purchased from Sinopharm (Shanghai, China). Sodium butylnaphthalenesulfonate was purchased from Adamas Beta (Shanghai, China). PEPG ($M_w = 4400$) and iron(III) p-toluenesulfonate hexahydrate were purchased from Siama-Aldrich (St Louis, MO, USA). Hydrochloric acid ethanol solution was purchased from Shenzhen Ketianhuabo Instrument Co. Ltd. (Shenzhen, China). All materials were used without further purification.

Polymerization

The details of the synthesis of the various ferric salts are given in the Supplementary Information. The polymerization can be conducted through two different methods, CP and VPP. In the CP method, the oxidative solution was mixed with EDOT at a molar ratio of 1:2.25 and then spin-cast at 2000–8000 r.p.m. for 15 s onto an 18 × 18 mm glass substrate pretreated with H_2O_2/H_2SO_4 solution. Next, the substrate was transferred to a hot plate and heated at 70 °C. In the VPP method, the oxidative solution was spin-cast at 2000–8000 r.p.m. for 15 s on the glass substrate. The coated substrate was then exposed to EDOT vapor in a quartz reaction chamber with constant argon flow and heated at 70–90 °C. After polymerization, the samples were washed with ethanol and dried in ambient temperature.

Reduction of PEDOT films

To adjust the reducing ability, 0.1 M phenylhydrazine ethanol solution was acidified with different amounts of dodecylbenzenesulfonic acid (from 0.16 to 0 M). The pristine PEDOT films were immersed in various reductant solutions for 10 min at room temperature (25 °C), and the reduced film was washed with ethanol and deionized water.

Characterization

The film resistance was measured by the Van der Pauw method using a Hall measurement system (HL5500PC). The film thickness was measured by a profilometer (DEKTAK-150). The S values were measured by two R-type thermocouples monitoring both the temperature difference and Seebeck voltage of the sample, which was heated on one side using a temperature-adjustable heating coil. The Raman spectra (Horiba Xplora One 532 nm) were used to confirm the structure and the doping states of PEDOT. The UV–Vis–NIR spectra (Varian Cary 5000) were used to determine the carrier types of the PEDOT films. A scanning electron microscope (Zeiss Supra S5) and an atomic force microscope (Veeco Dimension Icon) were used to observe the surface morphology of the PEDOT films. An energy dispersive spectrometer was used for elemental analysis. The doping level of PEDOT was determined using X-ray photoelectron spectroscopy (XPS; ESCAlab 250). The crystal structures of the film were characterized using grazing incidence X-ray diffraction

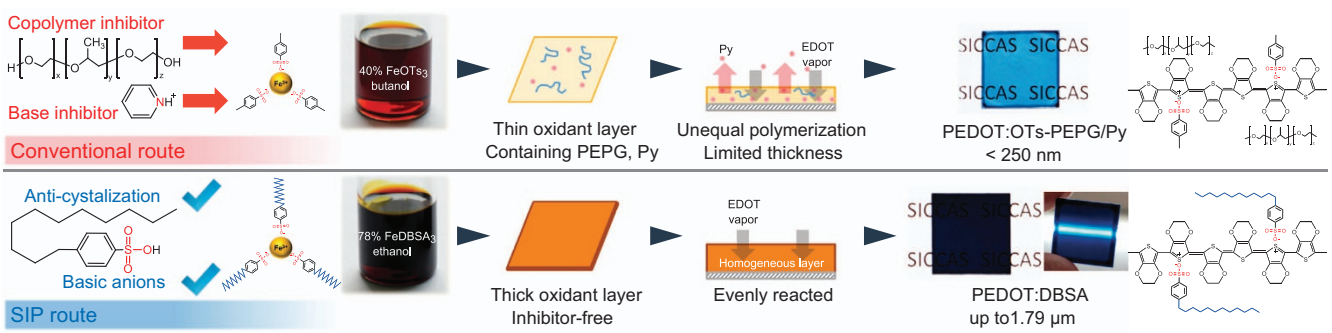

Scheme 1 A comparison of the conventional PEPG/Py-inhibited polymerization of PEDOT:OTs and the inhibitor-free SIP route-fabricating PEDOT:DBSA. The SIP route shows great advantages in simplicity, controllability and film thickness. DBSA, dodecylbenzenesulfonate; OT, tosylate; PEDOT, poly(3,4-ethylenedioxythiophene); PEPG, poly(ethylene glycol); SIP, self-inhibited polymerization.

(Rigaku D/max 2550 V). The temperature dependence of σ was measured using a system based on a thermal dilatometer (NETZSCH DIL 402PC), as previously reported.[37]

RESULTS AND DISCUSSION

Thickness and morphology

The precursor concentration, film thickness, reactivity and TE properties of the PEDOT films obtained using various oxidants are shown in Table 1 (additional examples in Supplementary Table S1). With the conventional oxidant $FeOTs_3$, the concentration is <40 wt %, and the maximum film thickness was 420 nm. To obtain high quality films, the use of inhibitors reduced the film thickness by at least 30% due to the concentrating effect.[33] In contrast, the inhibitor-free viscous coating solutions (>66 wt%) made by $FeCSA_3$, $FeBNSA_3$ and $FeDBSA_3$ enable the formation of high quality films with significantly increased thicknesses, >700 nm.

PEDOT polymerized without PEPG demonstrated greater homogeneity. Scanning electron microscope and atomic force microscope (Figures 1–c) show that both the PEDOT:OTs-PEPG/Py film (P1-d) and PEDOT:DBSA film (P4) have fairly flat surfaces (Rq ~ 5–7 nm) due to the shrinkage of the film during the drying process.[21] The energy dispersive spectrometer (Supplementary Figure S1) confirmed the single dopant of the two films. However, PEDOT:OTs-PEPG/Py exhibits a grain structure[28] and a cluster-shaped surface, which is likely caused by the phase separation of crystalline PEDOT:OTs[38] and the remaining PEPG that cannot be removed by solvents. PEPG-free PEDOT:DBSA films are homogeneous and have no distinguishable second phase. The existence of PEPG in the PEDOT:OTs was confirmed by XPS spectra (Figure 1d). Similar to Wang's report,[28] the XPS analysis of the PEDOT:OTs-PEPG/Py film shows a broad peak around 532.7 eV attributed to the oxygen atom from the remaining PEPG, masking the majority of the signals from PEDOT and its dopants. The elemental analysis by XPS (Figure 1e) shows a high concentration of oxygen, which also suggests a high content of nonconductive PEPG in the PEDOT:OTs. In comparison to conventional PEDOT:OTs, the PEPG-free PEDOT:DBSA film produced by the SIP method shows a very different O(*1s*) XPS spectrum. The oxygen signals of the thiophene unit (537–534 eV) and doping sulfonates (533–529 eV) are clearly observed. The intensity of the dopant signal significantly decreased after dedoping treatment (Supplementary Figure S3b).

σ and TE performance

The reaction completion time and $S^2\sigma$ of the PEDOT films obtained using different precursors are shown in Table 1. The polymerization completion time is affected by both the acidity of the anion and the addition of inhibitors. The polymerization using $FeOTs_3$ completed almost instantly without the use of an inhibitor, resulting in low-quality films. With the help of neutralization by pyridine and anti-crystallization/stabilization by PEPG, the $S^2\sigma$ of the obtained films significantly increased. This result confirms that the conventional oxidants could work only in combination with inhibitors to achieve viable films. Compared to conventional oxidants, the three new oxidants have more basic anions (pKa > -1.8).[39–42] Interestingly, the VPP time of PEDOT:DBSA and PEDOT:BNSA extends to >25 min and the CP time of PEDOT:CSA to 25 s. Because of the high basicity of the CSA and BNSA anions, extra acid is needed to accelerate the reaction (Supplementary Table S2). High $S^2\sigma$ was achieved in films obtained through mild reaction conditions using the oxidants containing WBAs, particularly $FeDBSA_3$, without any additives. The $S^2\sigma$ of the pristine PEDOT:DBSA film reached 69.6 $\mu W\,mK^{-2}$, higher than that of most of the reported pristine PEDOT films. In addition, the high solubility and low acidity of the new oxidants enable the polymerization in more kinds of solvents (such as methanol and ethanol) under various temperatures (Supplementary Tables S3 and S4), which also facilitates the synthesis.

Furthermore, σ is successfully maintained at a level of 1100 $S\,cm^{-1}$ over a wide range of film thicknesses (Figure 2), which indicates that

Table 1 Reactivity, TE performance and film thickness of PEDOT polymerized via different precursors

	Precursor composition and film thickness							*Reactivity and TE performance (298 K)*				
Method	*Anion*	*pKa*[a]	*Ox (wt%)*	*Py (wt%)*	*PEPG (wt%)*	*Extra acid (wt%)*	*Max. thickness (nm)*	*t (s)*	*σ (S cm⁻¹)*	*S (μV K⁻¹)*	*S²σ (μW mK⁻²)*	*Sample no. /ref.*
CP	OTs	−2.8[39]	20.0	0	0	0	80	0.5	19.3	13.2	0.336	P1-a
			19.7	1. 4↓	0	0	200	—	~300	~40	38	ref. 29
	CSA	1.2[39] (1.17[b])	66.7[c]	0	0	5. 0↑	700	25	752	26.4	52.4	P2
			70.2[c]	0	0	0	—	∞	—	—	—	—
VPP	OTs	−2.8[39]	40.0[d]	0	0	0	420	18	21	35.3	2.61	P1-b
			33.3[d]	0	16.7↓	0	280	300	589	22.4	29.6	P1-c
			33.0[d]	1. 1↓	16. 5↓	0	250	840	812	24.3	47.9	P1-d
			20.0	1.0↓	20.0↓	0	120	—	1550	14.9	34.4	ref. 28
	DBSA	−1.84[40,41] (−0.45[b])	78.1[e]	0	0	0	1790	1500	1140	24.7	69.6	P4
	BNSA	0.37[b]	68.6[d]	0	0	5.0↓	820	2100	200	26.7	14.3	P3
			72.2[d]	0	0	0	—	∞	—	—	—	—

Abbreviations: BNSA, butylnaphthalenesulfonate; CSA, camphorsulfonate; CP, casting polymerization; DBSA, dodecylbenzenesulfonate; OT, tosylate; Ox, oxidant; PEDOT, poly(3,4-ethylenedioxythiophene); PEPG, poly(ethylene glycol); Py, pyridine; TE, thermoelectric; VPP, vapor phase polymerization.
The maximum film thickness (±5 nm) and approximate reaction completion time (*t*, ±20%) are affected by the precursor composition including Ox, base inhibitor (Py), copolymer inhibitor (PEPG) and extra acid. Down arrow: inhibitors used to decrease the reaction rate. Up arrow: extra acid used to accelerate the reaction. ∞: non-reactive.
[a]Aqueous pKa value of corresponding acid.
[b]Calculated result by ACD Lab.[42]
[c]Maximum oxidant concentration at 25 °C. Too viscous to mix with monomer at higher concentration.
[d]Maximum oxidant concentration at 25 °C. Limited solubility.
[e]Maximum oxidant concentration at 25 °C. Too viscous for spin-coating at higher concentration.

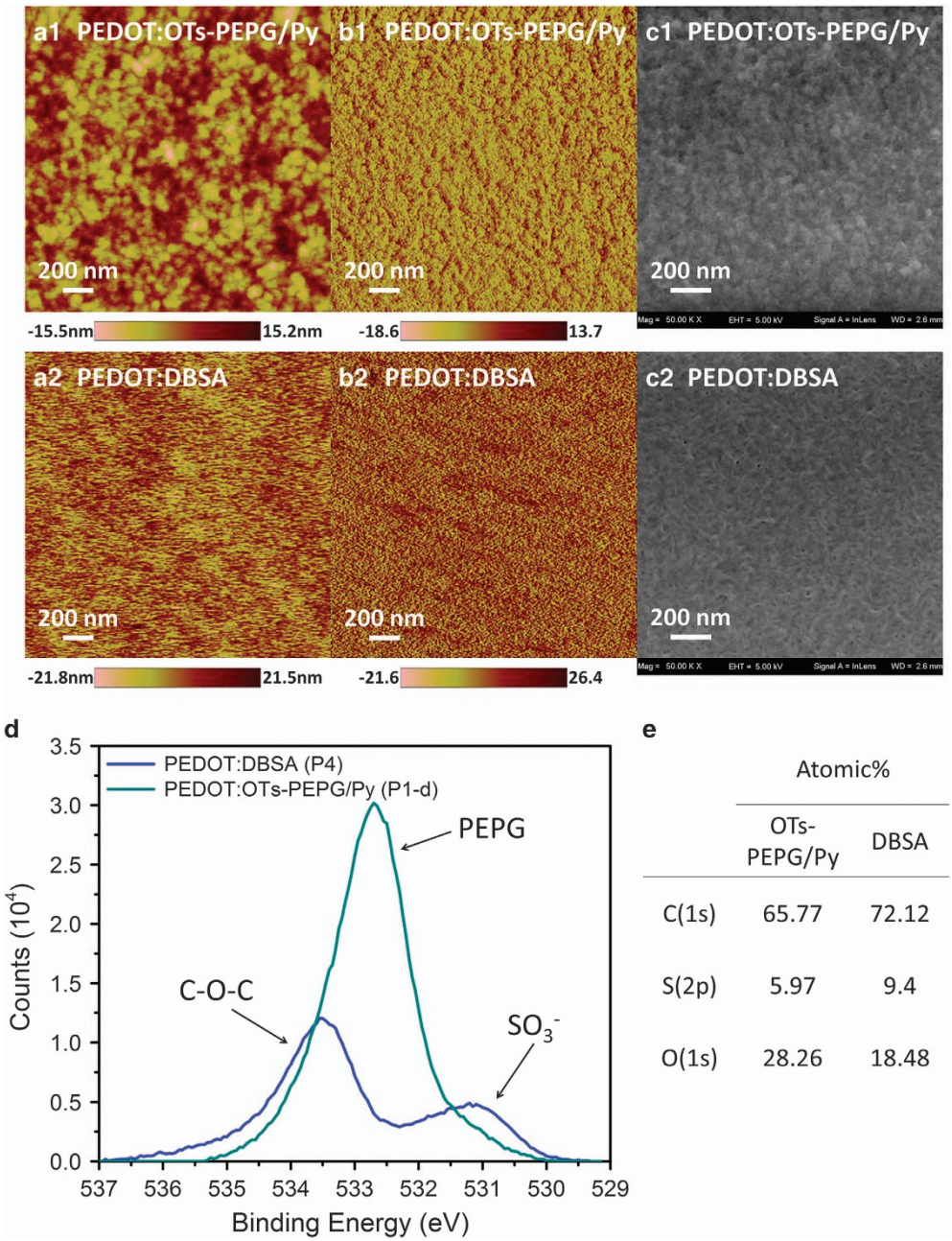

Figure 1 (**a**–**c**) AFM and SEM images of a 250 nm PEDOT:OTs-PEPG film ($a_1b_1c_1$, P1-d) and a 1240 nm PEDOT:DBSA film ($a_2b_2c_2$, P4). (a_1)&(a_2) Topographic images. (b_1)&(b_2) Phase images. (c_1)&(c_2) SEM images. (**d**) O(*1s*) XPS result of PEDOT films. (**e**) Elemental analysis by XPS. AFM, atomic force microscope; DBSA, dodecylbenzenesulfonate; OT, tosylate; PEDOT, poly(3,4-ethylenedioxythiophene); PEPG, poly(ethylene glycol); SEM, scanning electron microscope; XPS, X-ray photoelectron spectroscopy.

the reaction occurred evenly throughout the thick layer. Such thick films with low sheet resistance (down to 5 Ω) are potentially suitable for various applications such as flexible TE devices or electrode materials, while the PEDOT polymerized using conventional oxidants often suffers a drastic decrease in electrical performance with increasing film thickness due to the uneven evaporation of pyridine and the remaining PEPG.[27,31,33]

Effect of the anion on the reaction rate and doping level

To explain this self-inhibiting phenomenon, the role of the anion in the polymerization was investigated. According to previous experimental reports, the reaction rate (r_{total}) is influenced by the concentration of Fe^{3+} and H^+:[21]

$$r_{total} = k_1\left[Fe^{3+}\right]^2[EDOT]^2 + k_2[H^+]\left[Fe^{3+}\right][EDOT] \quad (1)$$

By using oxidants with WBAs, H^+ and Fe^{3+} concentrations can be kept at relatively low levels throughout the polymerization, effectively controlling the reaction rate. For example, in $c_{Fe} = 1$ M ideal aqueous solution containing just enough EDOT, the H^+ and Fe^{3+} concentrations and the corresponding reaction rates are shown in Figure 3 (see the calculation details in the Supplementary

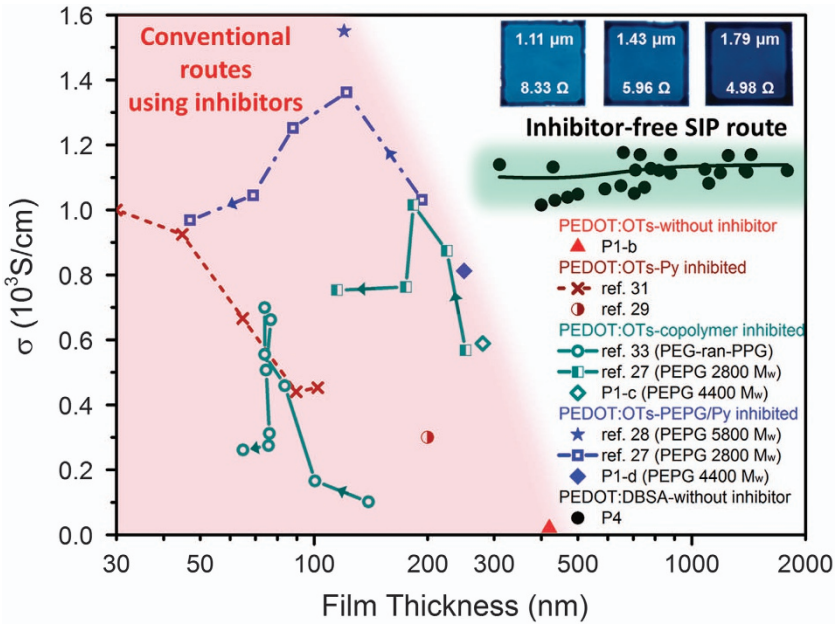

Figure 2 The film thickness dependence of σ. Arrow represents the increasing loading of copolymer that improves the σ at the sacrifice of film thickness. Images are taken under backlight to show the flat center parts. Thick margins were peeled off before measuring TE properties. TE, thermoelectric.

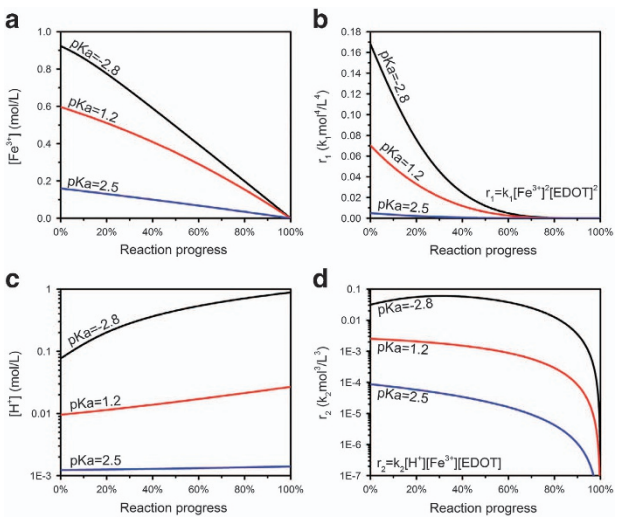

Figure 3 (**a**) Simulation of Fe^{3+} concentration change during the CP reaction process. (**b**) Rate of radical cation forming contributed by Fe^{3+}. (**c**) Simulation of H^+ concentration change during the reaction process. (**d**) Rate acceleration contributed by the catalytic effect of H^+. CP, casting polymerization.

Information). The initial reaction rate, contributed by Fe^{3+} (r_1), is reduced by ~50% when the pKa increases from −2.8 (OTs) to 1.2 (CSA) and further reduced (by ~93%) with a pKa change from 1.2 to 2.5; the pKa values of WBAs in alcohol are often increased by at least 2 compared to the aqueous value.[43] Furthermore, the acceleration phenomenon (r_2) caused by H^+ is also eliminated under high pKa conditions. In the VPP process, EDOT first dissolves in the precursor before reaction. The initial EDOT concentration and reaction rate are much lower, resulting in a much longer reaction time, but following a similar trend (Table 1). The SIP approach using oxidants containing WBAs exhibits controllable reaction rates and results in satisfactory film quality without the use of inhibitors. In contrast, rapid reaction using conventional oxidants causes a sharp decrease in the electrical property of the resultant film. Compared to the PEPG/pyridine-inhibited VPP sample of PEDOT:OTs, the directly VPP polymerized PEDOT:OTs without an inhibitor exhibits a poor σ of 21 S cm^{-1} (Table 1). Its higher S and dark appearance indicate a low-doping level.

The doping levels are characterized by combined analysis of XPS and Raman spectra data. The XPS S(*2p*) signals for sulfonates (170–166 eV) and thiophene units (166.5–162.5 eV) are different due to the different electronegativities of the neighboring atoms, and the ratio of the two signals reflects the doping level (Figure 4a).[25,26,29] The PEDOT:OTs synthesized using inhibitors have a doping level of 30.2%, almost twice the doping level (18.3%) of the sample polymerized rapidly without using an inhibitor. Surprisingly, the long-lasting SIP reaction of PEDOT:DBSA and PEDOT:BNSA using the VPP method results in extremely high doping levels of >42.9%, very close to the highest reported value (45.5%).[25] The SIP reaction of PEDOT:CSA using the CP method is not sufficiently stable (25 s) and achieves doping levels similar to PEPG/Py-inhibited polymerization of PEDOT:OTs. The doping level can also be reflected in the quinoid/benzoid ratio of the PEDOT chain.[44] Raman spectra (Figure 4b) were used to analyze the aromatic structure of PEDOT (see the overall data and vibration modes in Supplementary Figure S2). To compare the difference in aromatic absorbances, the spectra were normalized by taking the peak at 990 cm^{-1}, representing the oxyethylene ring deformation (including three peaks at 438, 573 and 990 cm^{-1}),[45] as the reference peak. The structure and the number of oxyethylene rings of PEDOT do not change with the doping states and thus these normalized peaks accurately represent the same amount of thiophene units. After normalization, we could compare the doping state using the intensities of the peaks at 1364 and 1429 cm^{-1} that reflect the benzoid structure of the PEDOT chain. This result shows that the rapidly polymerized PEDOT:OTs have a much greater percentage of the benzoid-type structure than the PEPG/Py-inhibited sample, indicating its lower doping level. The above XPS/Raman results

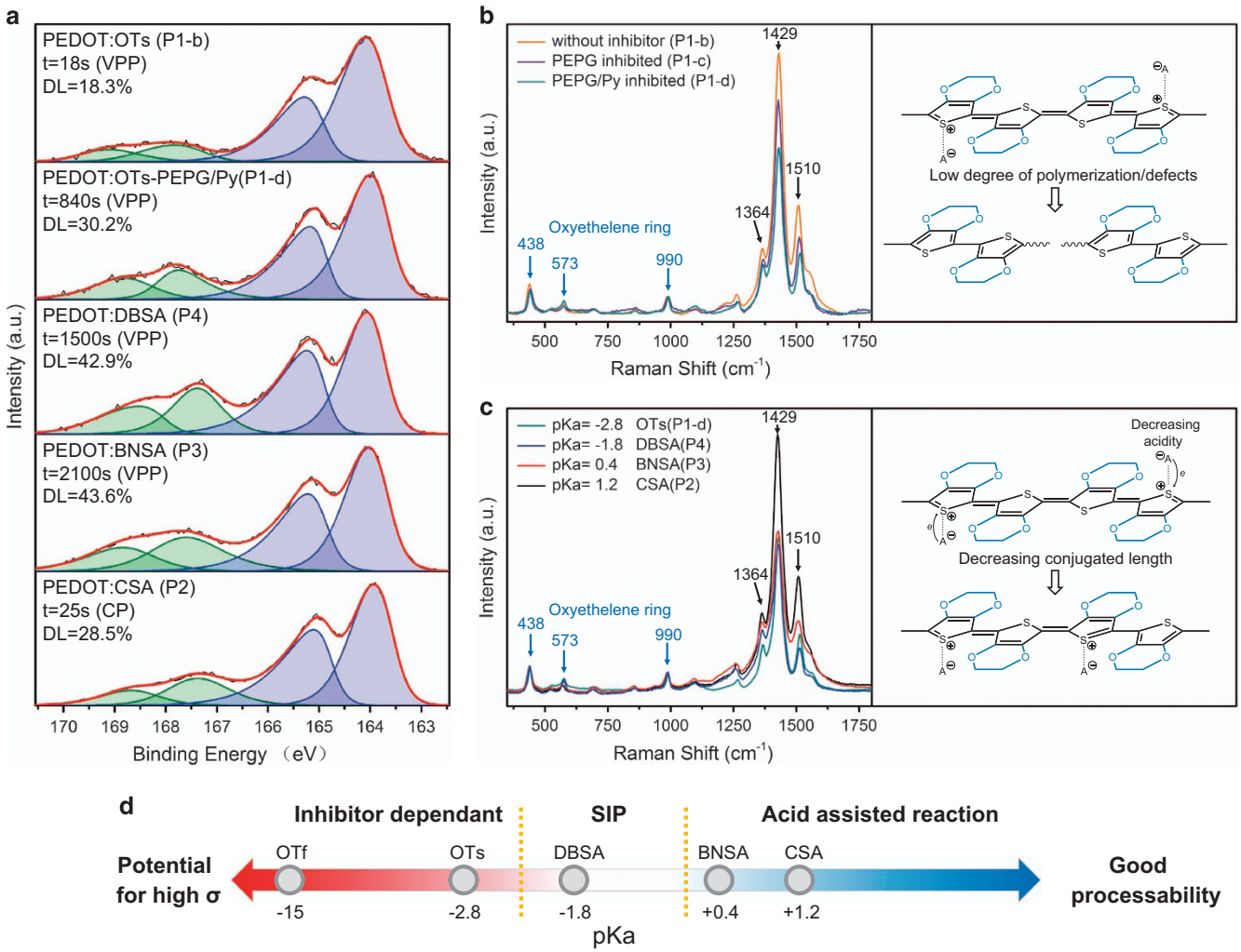

Figure 4 (**a**) S(*2p*) XPS result of PEDOT films showing DL under different reaction completion time (*t*). The doublet at high binding energy (170–166 eV) is from the sulfonate anions and the doublet at low energy (166.5–162.5 eV) is from the thiophene chain. The doping values are determined by the integral area ratio of two kinds of peaks ($r^2 > 0.996$). (**b**) Raman spectra of PEDOTs polymerized with/without inhibitors. Rapid reaction could cause defects-induced less doping-capable chains that resulted in sharp decrease of σ. (**c**) Raman spectra of PEDOTs doped with different counter-ions. The basicity-induced partial dedoping of PEDOT resulted in slight decrease of σ. (**d**) A schematic showing the two opposite effects of doping anion on the synthesis of PEDOT. DL, doping levels; PEDOT, poly(3,4-ethylenedioxythiophene); XPS, X-ray photoelectron spectroscopy.

indicate that rapid reaction can result in higher concentrations of defects or a lower degree of polymerization that prohibits the doping capability of thiophene chains.

Effect of the anion on the polymer structure and transport property

The basicity of the anion also has a considerable influence on chain conductance, which was also seen in the Raman spectra (Figure 4c). To further examine the effects, we synthesized four different PEDOT samples that were all polymerized under relatively mild conditions, resulting in doping levels higher than 28.5%. The intensity of the benzoid absorbance decreases with increasing acidity of the doping acid. Such a direct influence of counter-ion's basicity on the quinoid/benzoid ratio is even greater than the influence of the doping level. Even with a much higher doping level of 42.9%, PEDOT:DBSA still shows a lower percentage of conjugated structure than PEDOT:OTs (30.2% doping level). These results can be explained by the fact that with decreasing basicity of doping anions, the stabilization effect of positive charges created by the counter-ion is enhanced, which makes it possible to sustain a higher conjugated length in the bipolaron. It could also be said that the WBAs may partially donate their electrons to the thiophene rings and cause the dynamic balance to move slightly toward the benzoid-type structure. The use of PEDOT demands both good processability and performance, requiring a moderate basicity of the doping anion (Figure 4d).

The polycrystalline structures of the different PEDOT samples were observed using out-of-plane grazing incidence X-ray diffraction (Figure 5a). The peaks were indexed according to previous reports.[23,25,26] Such structures are formed after the rearrangement of polymer chains caused by the anisotropic shrinkage of the film during the drying process.[21] The ability to form fine crystals is determined by the steric effect of doping anions as well as the purity of PEDOT. A high degree of orientation was observed in all SIP samples, and only (h00) peaks were visible. The first peak appears at 6.3°, corresponding to the lamellar packing of PEDOT chains ($d = 13.93$ Å). Broader peaks with lower intensity were observed in PEDOT:CSA and PEDOT:BNSA, indicating increased structural disorder caused by large and rigid segments connected to SO_3^- that obstruct the crystal growth. The high crystallinity of PEDOT:DBSA is likely attributed to its smaller

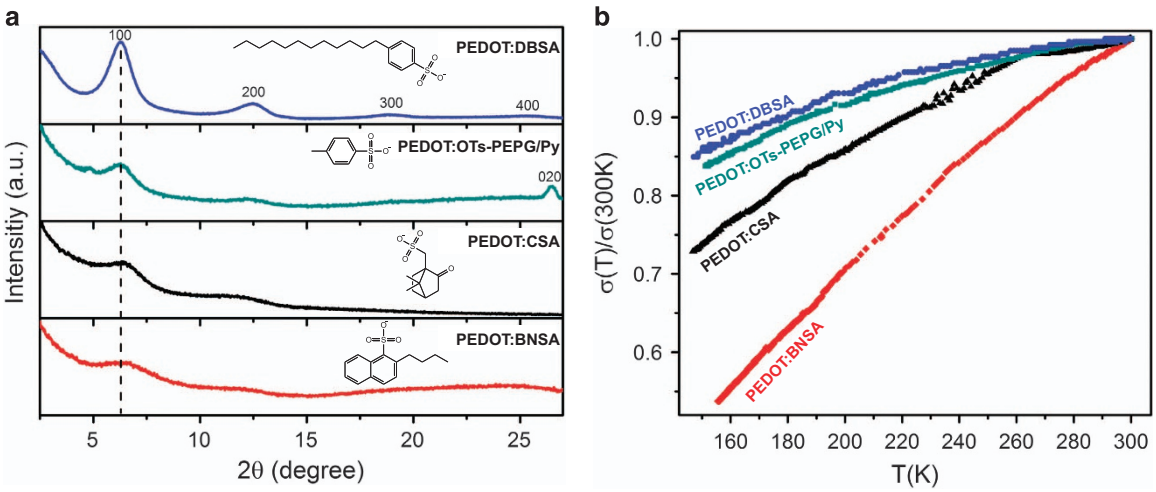

Figure 5 (**a**) Out-of-plane GIXRD diffractograms of PEDOT:DBSA, PEDOT:OTs-PEPG, PEDOT:CSA and PEDOT:BNSA. Angle of incidence: 0.4°. Scanning speed: 0.3° per min. (**b**) The temperature dependence of σ (normalized at 300 K) for PEDOT doped with anions of different steric effect. BNSA, butylnaphthalenesulfonate; CSA, camphorsulfonate; DBSA, dodecylbenzenesulfonate; GIXRD, grazing incidence X-ray diffraction; OT, tosylate; PEDOT, poly (3,4-ethylenedioxythiophene); PEPG, poly(ethylene glycol).

benzene segment and soft alkyl chains, which are able to fit in the free space without disturbing the crystal arrangements.

PEPG/Py-inhibited PEDOT:OTs has a moderate crystallinity. An additional (020) peak at 26.4° was observed, corresponding to the $\pi-\pi$ stacking of the thiophene rings ($d = 3.37$ Å), which cannot be detected by out-of-plane scattering in the samples prepared by SIP. This result indicates that the PEPG remaining in the polymer matrix may participate in the shrinking process and cause structural disorder and isotropic shrinkage due to its structural hindrance against the pulling of the substrate.

The increasing disorder of polymer chains generates localized states near the Fermi level that result in metal-Fermi glass transitions.[22] The decreased crystallinity results in a higher percentage of localized carriers. The change in slope in the σ versus T plot (Figure 5b) is consistent with the grazing incidence X-ray diffraction results. The naphthalene rings of PEDOT:BNSA are particularly rigid and have great steric hindrance, which lower its σ more than expected despite its high doping level of 43.6%.

Due to the lower basicity and the smaller anion size, PEDOT:OTs and PEDOT:OTf have exhibited potentially better electronic performance and higher σ in well-prepared films in previous reports.[25–28] However, the steric effect of nonconductive copolymer inhibitors and the challenge of controlling the polymerization should also be considered, particularly careful control of the film thickness. Therefore, PEDOT:DBSA seems to be a better option for applications due to its appropriate basicity, which ensures both good chain conductance and reaction control. The good solubility of $FeDBSA_3$ in alcohols and the inhibitor-free environment allow the fabrication of micron-thick homogeneous PEDOT films with high electrical performance through a facile one-step synthesis.

Optimization of $S^2\sigma$

In TE applications, $S^2\sigma$ can be optimized by dedoping PEDOT films with reductants such as TDAE,[29] hydrazine,[46] $NaBH_4$,[28] Na_2SO_3[47] and even strong alkalis such as NaOH.[44] In the present experiment, we used 0.1 M phenylhydrazine (PHZ), a mild and alcohol-soluble reducer, diluted with ethanol and acidified with different ratios of dodecylbenzenesulfonic acid to adjust the reducing ability of the reductant solution. According to the Nernst equation, the reducing potential increases with decreasing pH value, which is in turn determined by the acid/PHZ ratio. The PEDOT:DBSA film was immersed in the reductant solution at different acid/PHZ ratios to obtain PEDOT with different oxidation levels. As shown in Figure 6a, the electrical conductivities of the reduced films monotonously decreased with increasing S. The optimized $S^2\sigma$ of 77.2 μW mK^{-2} for the partly reduced film was obtained with an acid/PHZ ratio of 1.2. Supplementary Table S5 shows the calculated maximum power output of a single PEDOT film as a leg in a TE film module. Thick films with optimized power factors generate more power than the thin pristine films at the same temperature difference.

Figure 6b shows the UV–Vis–NIR spectra of pristine and dedoped PEDOT. $PEDOT^{2+}$ (bipolaron) chains exhibit a broad absorption band in the near infrared region. $PEDOT^{\cdot +}$ (polaron) and $PEDOT^0$ (neutral state) chains possess absorbance bands near 900 and 600 nm.[28,48,49] As the dedoping proceeded, the absorption near 600 nm increased, which was then followed by a decrease in the broad IR absorption, indicating that $PEDOT^{2+}$ was converted into neutral $PEDOT^0$. The absorption band near 900 nm increased at first and then decreased, indicating that a polaron is a metastable state of the carrier during the reduction process. The color of the films darkened with increasing absorbance near 600 nm in the visible light region (Figure 6c). This result coincides with the changes in the TE properties of the film. After being fully dedoped with pure phenylhydrazine (Acid/PHZ ratio = 0), the doping level of the PEDOT:DBSA decreased to 13.5% (Supplementary Figure S3a).

CONCLUSION

Novel oxidants ($FeCSA_3$, $FeBNSA_3$ and $FeDBSA_3$) with high solubility and WBAs were used in the synthesis of high quality micron-thick S-PEDOT films. The anions of these ferric salts exhibit self-inhibiting function during polymerization and can inhibit both the ionization of H^+ through their basicity and the crystallization of oxidants due to their alcohophilic structure. The thickness of the obtained homogeneous films reached the micron scale through a facile one-step synthesis using the heavy coating solution without an inhibitor. In addition, due to the appropriate anion basicity and low steric effect, the slow and even reaction between EDOT and the oxidant produced polycrystalline PEDOT:DBSA with an extremely

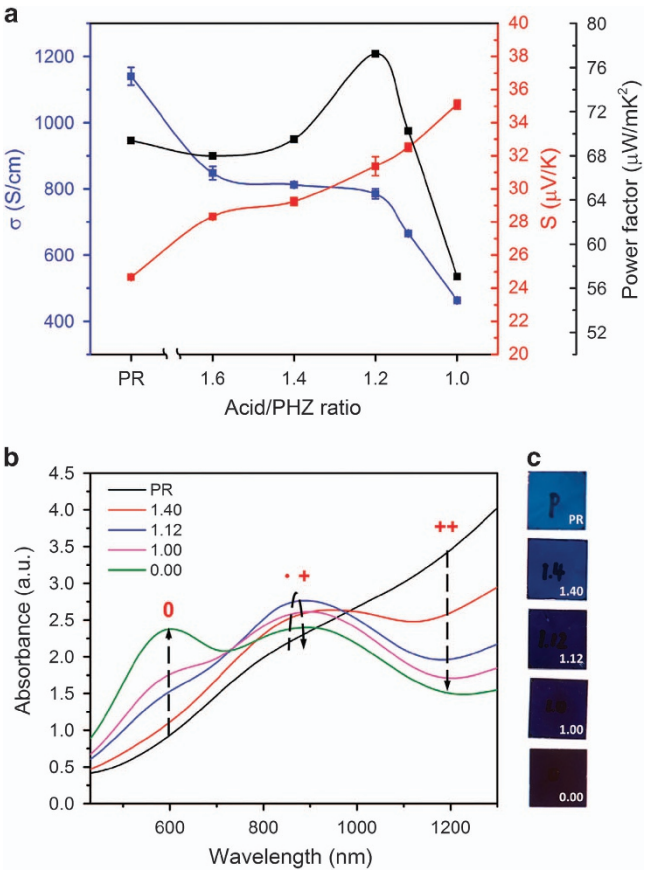

Figure 6 (**a**) TE property of the reduced films as a function of acid/PHZ ratio. (**b**) UV–Vis–NIR spectra of pristine PEDOT and reduced PEDOT with acid/PHZ ratio varied from 1.4–0. '0', '·+' and '++' stand for neutral state, polaron state and bipolaron state, respectively. (**c**) Changing in color of the reduced film. PEDOT, poly(3,4-ethylenedioxythiophene); TE, thermoelectric.

high doping level of 42.9%, a high σ of ~1100 S cm^{-1}, and film thicknesses as great as 1.79 μm. The $S^2\sigma$ of the pristine film reached 69.4 μW mK^{-2} and was able to be further optimized by reduction. This facile approach introduces great possibilities for the development of new functional PEDOT materials through anion design and the development of homogeneous thick films with high electrical conductivity for practical applications.

CONFLICT OF INTEREST

The authors declare no conflict of interest.

ACKNOWLEDGEMENTS

This work was supported by the National Key Research and Development Program of China (No 2016YFA0201103), a research grant from the Shanghai Government (No 15JC1400301) and the National Natural Science Foundation of China (No 51632010).

1 Yao, Q., Wang, Q., Wang, L., Wang, Y., Sun, J., Zeng, H., Jin, Z., Huang, X. & Chen, L. The synergic regulation of conductivity and Seebeck coefficient in pure polyaniline by chemically changing the ordered degree of molecular chains. *J. Mater. Chem. A* **2**, 2634 (2014).
2 Kemp, N. T., Kaiser, A. B., Trodahl, H. J., Chapman, B., Buckley, R. G., Partridge, A. C. & Foot, P. J. S. Effect of ammonia on the temperature-dependent conductivity and thermopower of polypyrrole. *J. Polym. Sci., Part B: Polym. Phys.* **44**, 1331–1338 (2006).
3 Zhang, Q., Sun, Y., Xu, W. & Zhu, D. Thermoelectric energy from flexible P3HT films doped with a ferric salt of triflimide anions. *Energy. Environ. Sci.* **5**, 9639 (2012).
4 Sun, Y., Sheng, P., Di, C., Jiao, F., Xu, W., Qiu, D. & Zhu, D. Organic thermoelectric materials and devices based on p- and n-type poly(metal 1,1,2,2-ethenetetrathiolate)s. *Adv. Mater.* **24**, 932–937 (2012).
5 See, K. C., Feser, J. P., Chen, C. E., Majumdar, A., Urban, J. J. & Segalman, R. A. Water-processable polymer-nanocrystal hybrids for thermoelectrics. *Nano Lett.* **10**, 4664–4667 (2010).
6 Coates, N. E., Yee, S. K., McCulloch, B., See, K. C., Majumdar, A., Segalman, R. A. & Urban, J. J. Effect of interfacial properties on polymer-nanocrystal thermoelectric transport. *Adv. Mater.* **25**, 1629–1633 (2013).
7 Yee, S. K., Coates, N. E., Majumdar, A., Urban, J. J. & Segalman, R. A. Thermoelectric power factor optimization in PEDOT:PSS tellurium nanowire hybrid composites. *Phys. Chem. Chem. Phys.* **15**, 4024–4032 (2013).
8 Du, Y., Cai, K. F., Chen, S., Cizek, P. & Lin, T. Facile preparation and thermoelectric properties of $Bi_{(2)}Te_{(3)}$ based alloy nanosheet/PEDOT:PSS composite films. *ACS Appl. Mater. Interfaces* **6**, 5735–5743 (2014).
9 Zhang, B., Sun, J., Katz, H. E., Fang, F. & Opila, R. L. Promising thermoelectric properties of commercial PEDOT:PSS materials and their bi2Te3 powder composites. *ACS Appl. Mater. Interfaces* **2**, 3170–3178 (2010).
10 Toshima, N. & Jiravanichanun, N. Improvement of thermoelectric properties of PEDOT/PSS films by addition of gold nanoparticles: enhancement of Seebeck coefficient. *J. Electron. Mater.* **42**, 1882–1887 (2013).
11 Kim, G. H., Shao, L., Zhang, K. & Pipe, K. P. Engineered doping of organic semiconductors for enhanced thermoelectric efficiency. *Nat. Mater.* **12**, 719–723 (2013).
12 Zheng, M., Huo, J., Chen, B., Tu, Y., Wu, J., Hu, L. & Dai, S. Pt–Co and Pt–Ni hollow nanospheres supported with PEDOT:PSS used as high performance counter electrodes in dye-sensitized solar cells. *Solar Energy* **122**, 727–736 (2015).
13 Sun, Y., Yang, Z., Gao, P., He, J., Yang, X., Sheng, J., Wu, S., Xiang, Y. & Ye, J. Si/PEDOT:PSS hybrid solar cells with advanced antireflection and back surface field designs. *Nanoscale Res. Lett.* **11**, 356 (2016).
14 Liu, Y., Feng, J., Ou, X., Cui, H., Xu, M. & Sun, H. Ultrasmooth, highly conductive and transparent PEDOT:PSS/silver nanowire composite electrode for flexible organic light-emitting devices. *Org. Electron.* **31**, 247–252 (2016).
15 Kim, Y. H., Wolf, C., Cho, H., Jeong, S. H. & Lee, T. W. Highly efficient, simplified, solution-processed thermally activated delayed-fluorescence organic light-emitting diodes. *Adv. Mater.* **28**, 734–741 (2016).
16 Zhang, C., Higgins, T. M., Park, S., O'Brien, S. E., Long, D., Coleman, J. N. & Nicolosi, V. Highly flexible and transparent solid-state supercapacitors based on RuO2/PEDOT:PSS conductive ultrathin films. *Nano Energy* **28**, 495–505 (2016).
17 Cheng, T., Zhang, Y., Zhang, J., Lai, W. & Huang, W. High-performance free-standing PEDOT:PSS electrodes for flexible and transparent all-solid-state supercapacitors. *J. Mater. Chem. A* **4**, 10493–10499 (2016).
18 Wang, J., Karmakar, R. S., Lu, Y., Wu, M. & Wei, K. Nitrogen plasma surface modification of poly(3,4-ethylenedioxythiophene):poly(styrenesulfonate) films to enhance the piezoresistive pressure-sensing properties. *J. Phys. Chem. C* **120**, 25977–25984 (2016).
19 Vuorinen, T., Niittynen, J., Kankkunen, T., Kraft, T. M. & Mantysalo, M. Inkjet-printed graphene/PEDOT:PSS temperature sensors on a skin-conformable polyurethane substrate. *Sci. Rep.* **6**, 35289 (2016).
20 Nardes, A. M., Kemerink, M. & Janssen, R. A. J. Anisotropic hopping conduction in spin-coated PEDOT:PSS thin films. *Phys. Rev. B* **76** (2007).
21 Elschner, A., Kirchmeyer, S., Lövenich, W., Merker, U. & Reuter, K. *Principles and Applications of an Instrinsically Conductive Polymer* (Taylor & Francis Group, 2011).
22 Bubnova, O., Khan, Z. U., Wang, H., Braun, S., Evans, D. R., Fabretto, M., Hojati-Talemi, P., Dagnelund, D., Arlin, J. B., Geerts, Y. H., Desbief, S., Breiby, D. W., Andreasen, J. W., Lazzaroni, R., Chen, W. M., Zozoulenko, I., Fahlman, M., Murphy, P. J., Berggren, M. & Crispin, X. Semi-metallic polymers. *Nat. Mater.* **13**, 190–194 (2014).
23 Aasmundtveit, K. E., Samuelsen, E. J., Pettersson, L. A. A., Inganäs, O., Johansson, T. & Feidenhans'l, R. Structure of thin films of poly(3,4-ethylenedioxythiophene). *Synth. Met.* **101**, 561–564 (1999).
24 Shi, W., Zhao, T., Xi, J., Wang, D. & Shuai, Z. Unravelling doping effects on PEDOT at the molecular level: from geometry to thermoelectric transport properties. *J. Am. Chem. Soc.* **137**, 12929–12938 (2015).
25 Massonnet, N., Carella, A., de Geyer, A., Faure-Vincent, J. & Simonato, J. Metallic behaviour of acid doped highly conductive polymers. *Chem. Sci.* **6**, 412–417 (2015).
26 Gueye, M. N., Carella, A., Massonnet, N., Yvenou, E., Brenet, S., Faure-Vincent, J., Pouget, S., Rieutord, F., Okuno, H., Benayad, A., Demadrille, R. & Simonato, J. Structure and dopant engineering in PEDOT thin films: practical tools for a dramatic conductivity enhancement. *Chem. Mater.* **28**, 3462–3468 (2016).
27 Park, T., Park, C., Kim, B., Shin, H. & Kim, E. Flexible PEDOT electrodes with large thermoelectric power factors to generate electricity by the touch of fingertips. *Energy. Environ. Sci.* **6**, 788 (2013).
28 Wang, J., Cai, K. & Shen, S. A facile chemical reduction approach for effectively tuning thermoelectric properties of PEDOT films. *Org. Electron.* **17**, 151–158 (2015).
29 Bubnova, O., Khan, Z. U., Malti, A., Braun, S., Fahlman, M., Berggren, M. & Crispin, X. Optimization of the thermoelectric figure of merit in the conducting polymer poly(3,4-ethylenedioxythiophene). *Nat. Mater.* **10**, 429–433 (2011).

30 Winther-Jensen, B., Breiby, D. W. & West, K. Base inhibited oxidative polymerization of 3,4-ethylenedioxythiophene with iron(III)tosylate. *Synth. Met* **152**, 1–4 (2005).
31 Levermore, P. A., Chen, L., Wang, X., Das, R. & Bradley, D. D. C. Fabrication of highly conductive poly(3,4-ethylenedioxythiophene) films by vapor phase polymerization and their application in efficient organic light-emitting diodes. *Adv. Mater.* **19**, 2379–2385 (2007).
32 Mueller, M., Fabretto, M., Evans, D., Hojati-Talemi, P., Gruber, C. & Murphy, P. Vacuum vapour phase polymerization of high conductivity PEDOT: Role of PEG-PPG-PEG, the origin of water, and choice of oxidant. *Polymer* **53**, 2146–2151 (2012).
33 Fabretto, M., Müller, M., Zuber, K. & Murphy, P. Influence of PEG-ran-PPG surfactant on vapour phase polymerised PEDOT thin films. *Macromol. Rapid Commun.* **30**, 1846–1851 (2009).
34 Fabretto, M., Zuber, K., Hall, C., Murphy, P. & Griesser, H. J. The role of water in the synthesis and performance of vapour phase polymerised PEDOT electrochromic devices. *J. Mater. Chem.* **19**, 7871 (2009).
35 Winther-Jensen, B., Fraser, K., Ong, C., Forsyth, M. & MacFarlane, D. R. Conducting polymer composite materials for hydrogen generation. *Adv. Mater.* **22**, 1727–1730 (2010).
36 Anno, H., Nishinaka, T., Hokazono, M., Oshima, N. & Toshima, N. Thermoelectric power-generation characteristics of PEDOT:PSS thin-film devices with different thicknesses on polyimide substrates. *J. Electron. Mater.* **44**, 2105–2112 (2015).
37 Liu, H., Shi, X., Xu, F., Zhang, L., Zhang, W., Chen, L., Li, Q., Uher, C., Day, T. & Snyder, G. J. Copper ion liquid-like thermoelectrics. *Nat. Mater.* **11**, 422–425 (2012).
38 Kim, J., Kim, E., Won, Y., Lee, H. & Suh, K. The preparation and characteristics of conductive poly(3,4-ethylenedioxythiophene) thin film by vapor-phase polymerization. *Synth. Met.* **139**, 485–489 (2003).
39 Xiao, D., Zhang, S., Zhang, D., Xie, D., Zeng, Q., Xiang, Y., Ning, R., Li, X. & Jin, W. Reversible transformation of self-assemblies and fluorescence by protonation-deprotonation in pyrimidinylene-phenylene macrocycles. *Chem. Commun.* **52**, 4357–4360 (2016).
40 Sagi, K. V., Amanapu, H. P., Teugels, L. G. & Babu, S. V. Investigation of guanidine carbonate-based slurries for chemical mechanical polishing of Ru/TiN barrier films with minimal corrosion. *ECS . Solid State Sci. Technol.* **3**, P227–P234 (2014).
41 Finnie, A. A., Price, C. & Ramsden, R. A. Polymer with salt groups and antifouling coating composition comprising said polymer. European Patent EP 2313466 A1 (2011).
42 ACD/I-Lab 2.0. Available at: https://ilab.acdlabs.com/iLab2/. Accessed on December 2015.
43 Brauer, G. M., Durany, G. & Argentar, H. Ionization constants of substituted benzoic acids in ethanol-water. *J. Res. Natl Bur. Stand. A. Phys. Chem.* **71A**, 379–384 (1967).
44 Tsai, T., Chang, H., Chen, C., Huang, Y. & Whang, W. A facile dedoping approach for effectively tuning thermoelectricity and acidity of PEDOT:PSS films. *Org. Electron.* **15**, 641–645 (2014).
45 Garreau, S., Louarn, G., Buisson, J. P., Froyer, G. & Lefrant, S. *In situ* spectroelectrochemical Raman studies of poly(3,4-ethylenedioxythiophene) (PEDT). *Macromolecules* **32**, 6807–6812 (1999).
46 Lee, S. H., Park, H., Kim, S., Son, W., Cheong, I. W. & Kim, J. H. Transparent and flexible organic semiconductor nanofilms with enhanced thermoelectric efficiency. *J. Mater. Chem. A* **2**, 7288 (2014).
47 Massonnet, N., Carella, A., Jaudouin, O., Rannou, P., Laval, G., Celle, C. & Simonato, J. Improvement of the Seebeck coefficient of PEDOT:PSS by chemical reduction combined with a novel method for its transfer using free-standing thin films. *J. Mater. Chem. C* **2**, 1278–1283 (2014).
48 Garreau, S., Duvail, J. L. & Louarn, G. Spectroelectrochemical studies of poly(3,4-ethylenedioxythiophene) in aqueous medium. *Synth. Met.* **125**, 325–329 (2002).
49 Zhang, F., Götz, G., Mena-Osteritz, E., Weil, M., Sarkar, B., Kaim, W. & Bäuerle, P. Molecular and electronic structure of cyclo[10]thiophene in various oxidation states: polaron pair vs. bipolaron. *Chem. Sci.* **2**, 781 (2011).

Supplementary Information accompanies the paper on the NPG Asia Materials website (http://www.nature.com/am)